Check for updates

An amide hydrogen bond templated [1]rotaxane displaying a peptide motif – demonstrating an expedient route to synthetic mimics of lasso peptides†‡

Matthew J. Young, [ID] § Geoffrey R. Akien [ID] and Nicholas H. Evans [ID] *

The rapid synthesis of an amide hydrogen bond templated [1]rotaxane is reported – demonstrating a potential pathway to synthetic analogues of lasso peptides. The structures of the [1]rotaxane and its unthreaded isomer have been characterized by NMR spectroscopy and modelled using DFT calculations.

Introduction

Lasso peptides are a fascinating class of structurally unusual peptides consisting of a polypeptide chain that threads its "tail" through a macrolactam "ring" (Fig. 1).[1] Due to their entangled structure, lasso peptides have been found to evade degradation by enzymes, and examples have been shown to possess a number of useful bioactive characteristics, including antimicrobial activity,[2] receptor antagonism[3] and enzyme inhibition.[4] The total synthesis of lasso peptides is in its infancy, with the first chemical synthesis of a lasso peptide having only very recently been reported.[5] However, it has been established that the conformationally constrained amino acids displayed in the "loop region" (see Fig. 1) are important in determining the biological activity of a lasso peptide.[6] Synthetic [1]rotaxanes[7] are structurally equivalent to lasso peptides, but examples that display peptide sequences are rare.[8,9]

Recently we have rapidly prepared [2]rotaxanes[10–12] by use of hydrogen bond templation[13] and CuAAC click chemistry to stopper a simple amide half-axle component threaded through an isophthalamide macrocycle.[14] Here we are reporting an adaptation of this method to rapidly prepare a [1]rotaxane displaying a Gly–Gly–Gly–Gly peptide sequence within the key loop region, by appending and then cyclizing a peptide chain on a novel "scaffold" [2]rotaxane. Successful preparation of the target [1]rotaxane was confirmed by NMR spectroscopy and mass spectrometry. Structural comparison with the non-interlocked isomer of the [1]rotaxane has also been undertaken by NMR spectroscopy and DFT calculations.

When compared to prior work from the laboratories of Coutrot[8] and Bode,[9] the synthetic route reported here has the potential to generate better mimics of naturally occurring lasso peptides. In the previous cases, the entangled structure arises from the non-amide templation of a protonated ammonium passing through a 24-crown-8 macrocycle. Here, amide motifs (used to template formation of the interlocked structure through the carbonyl O atom of the axle to the isophthalamide N–Hs of the macrocycle) are to be found in both the axle and ring components – not just the peptide sequence in the loop region.
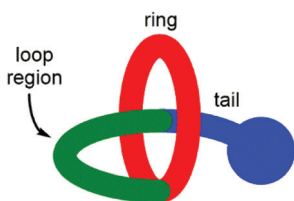

Fig. 1 Schematic representation of structure of a lasso peptide and [1] rotaxane.

Department of Chemistry, Lancaster University, Lancaster, LA1 4YB, UK.
E-mail: n.h.evans@lancaster.ac.uk

†Underlying data for this paper are provided in the Experimental section and ESI,‡ along with electronic copies of NMR spectra (including fid files) and computational output files being available from: DOI: 10.17635/lancaster/research-data/372.
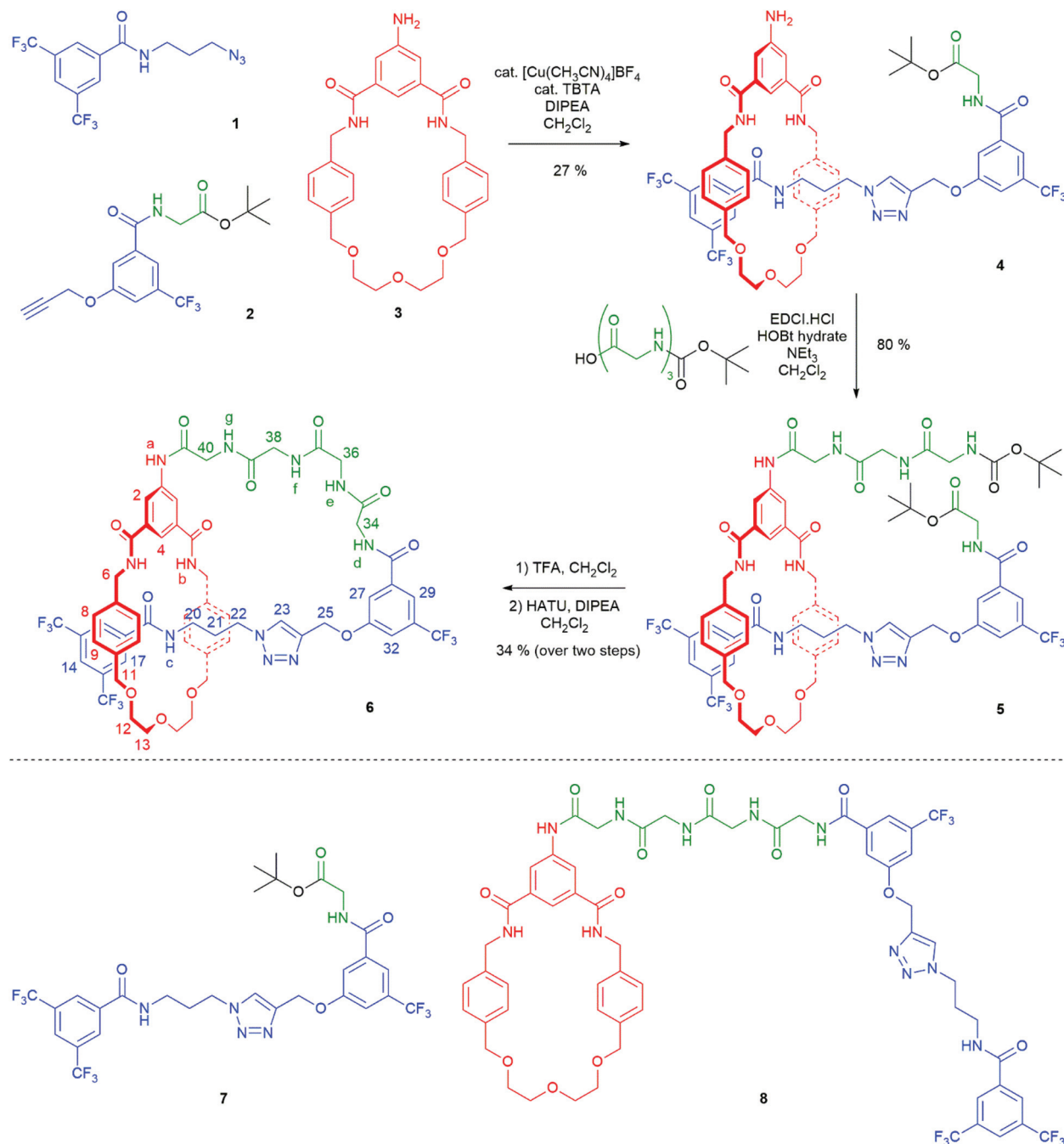
§Current address: Institute of Organic Chemistry, Albert-Ludwigs-University of Freiburg, Albertstrasse 21, 79104 Freiburg, Germany.

Results and discussion

The synthesis of [1]rotaxane **6** is presented in Scheme 1. All novel compounds were characterized by NMR spectroscopy (¹H, ¹³C and where applicable ¹⁹F), IR spectroscopy and high resolution mass spectrometry. Scaffold [2]rotaxane **4** was prepared using azide **1**, alkyne **2** and amino macrocycle **3**. Azide **1** was synthesized according to our previously reported pro-

This journal is © The Royal Society of Chemistry 2020

Org. Biomol. Chem., 2020, **18**, 5203–5209 | **5203**

Scheme 1 Synthesis of tetra-glycine [1]rotaxane **6** *via* "scaffold" [2]rotaxane **4**, and structures of axle **7** and unthreaded "[1]rotaxane" isomer **8**.

cedures in two chromatography-free steps.[10] Novel alkyne **2** was prepared in four chromatography-free steps (see ESI, page S3‡), with inclusion of a glycine unit as part of **2** to guarantee sufficient bulk for the rotaxane stopper. Novel amino macrocycle **3** was synthesized in four steps from commercially available starting materials (see ESI, pages S6 & S9‡).¶

¶Single crystals of macrocycle **3** suitable for X-ray structure determination were obtained by slow evaporation of a chloroform/methanol solution. The solved structure (CCDC 1995143‡) and further details are to be found in ESI, page S50.‡

[2]Rotaxane **4** was synthesized using our recently reported hydrogen bond templated strategy.[10–12] Macrocycle **3** was dissolved in CH_2Cl_2 in the presence of 1.1 equivalents of azide **1** and 1.1 equivalents of alkyne **2**. Catalytic $[Cu(CH_3CN)_4]BF_4$ and TBTA and 1.2 equivalents of DIPEA were added and the reaction stirred overnight at room temperature under an inert atmosphere. After aqueous work-up and careful silica chromatography, [2]rotaxane **4** was isolated in 27% yield.[15]

The ^{1}H NMR spectra of [2]rotaxane **4**, along with that of non-interlocked macrocycle **3** and axle **7** (for synthesis of axle

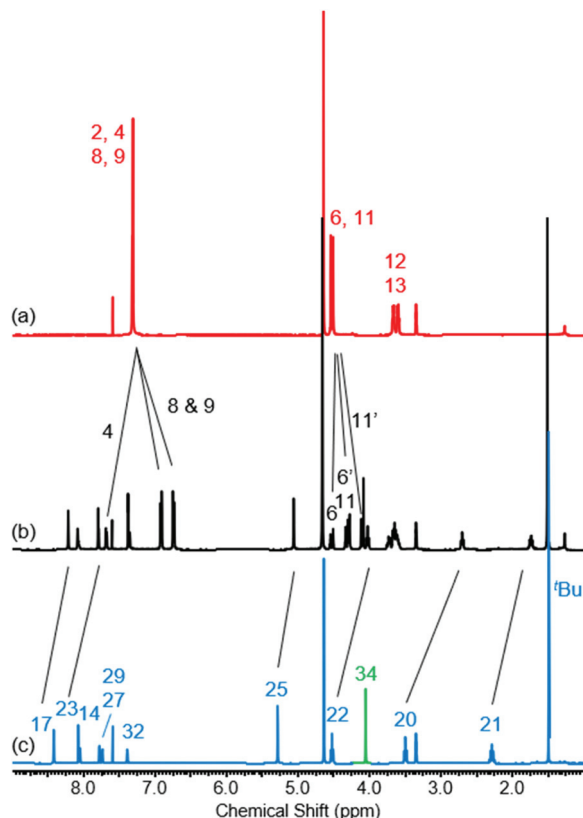**5204** | *Org. Biomol. Chem.*, 2020, **18**, 5203–5209

This journal is © The Royal Society of Chemistry 2020

Fig. 2 ^{1}H NMR spectra of (a) macrocycle **3**, (b) [2]rotaxane **4** and (c) axle **7** (1:1 CDCl3/CD3OD, 400 MHz, 298 K). For atom labels see Scheme 1.

Fig. 3 ^{1}H NMR spectra of (a) [1]rotaxane **6** and (b) unthreaded isomer **8** (D6-DMSO, 400 MHz, 298 K). For atom labels see Scheme 1.

7 see ESI, page S30‡) are shown in Fig. 2. The upfield shift and splitting of aromatic macrocycle protons *8* and *9* and the upfield shifts of axle protons *17*, *20*, *21*, *22*, *23* and *25* in [2]rotaxane **4** compared to macrocycle **3** and axle **7** are consistent with the threading of the axle component through the macrocycle. The downfield shift of internal isophthalamide proton *4* is indicative of hydrogen bonding to the carbonyl oxygen of the axle amide. Evidence to support the co-conformation of [2]rotaxane **4** depicted in Scheme 1 is provided by the appearance of through-space correlations in the ^{1}H ROESY NMR spectrum between protons *8* and *9* of the macrocycle and axle proton environments *17*, *20* and *21* (see ESI, page S16‡). For [2]rotaxane **4**, the resonances of macrocyclic protons *6* and *11* are split due to the directionality of the threaded axle that causes the protons attached to the same carbon to become inequivalent. In addition, the molecular ion peak [M + Na]+ for [2]rotaxane **4** was observed in the positive-ion electrospray mass spectrum at m/z = 1209 Da (see ESI, page S17‡).

With [2]rotaxane **4** in-hand, preparation of the target [1] rotaxane was executed. Boc–Gly–Gly–Gly was appended to the macrocyclic amine group of [2]rotaxane **4** by use of EDC coupling in 80% yield (using three equivalents of the protected tripeptide). Treatment of Boc-peptide appended [2]rotaxane **5** with TFA in CH2Cl2 simultaneously removed both the Boc and *tert*-butyl ester. Cyclization was carried out using HATU[16] at a
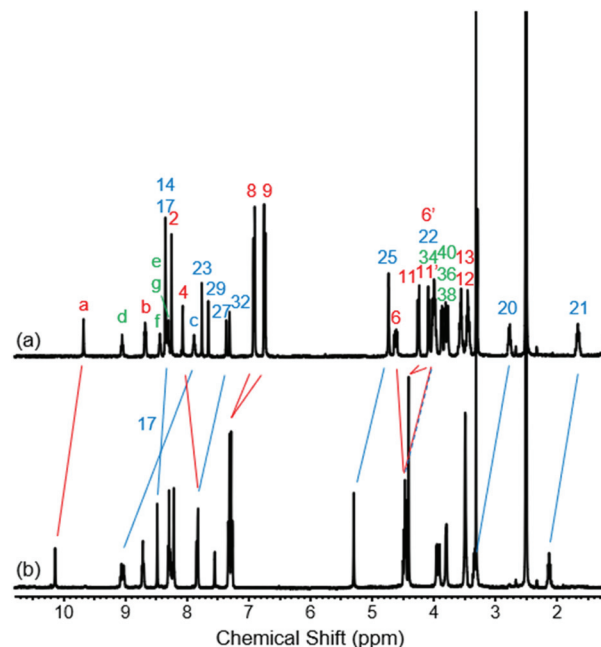
dilute concentration of 2 mmol L−1 of deprotected **5** in CH2Cl2 to minimize the effect of competing oligomerization reactions, with [1]rotaxane **6** being isolated in 34% yield (over two steps from **5**) after aqueous work-up and silica gel column chromatography. Confirmation of the successful isolation of target [1] rotaxane **6** was ascertained by NMR spectroscopy and mass spectrometry – a molecular ion peak [M + Na]+ for **6** being observed in the positive-ion electrospray mass spectrum at m/z = 1306 Da (see ESI, page S24‡).

To study the structural effects of [1]rotaxane **6** being interlocked, the unthreaded analogue **8** was also prepared (for details of synthesis see ESI, page S33‡). Inspection of the ^{1}H NMR spectra (recorded in D6-DMSO due to the very limited solubility of **8**, Fig. 3) reveals the anticipated shielding of protons *8*, *9*, *17*, *20*, *21*, *22* and *25* (but interestingly not *23*) and deshielding of proton *4* for [1]rotaxane **6** compared to unthreaded **8**. In addition, the axle amide proton *c* is notably upfield in **6** compared to **8**, consistent to being present within the shielding macrocyclic cavity of [1]rotaxane **6**. There is also the expected marked splitting of macrocyclic resonances *6* and *11* for [1]rotaxane **6** arising from the directionality of the threaded axle. Other notable differences in chemical shift between the two molecules are for amide proton *a* (significantly greater than for any of the glycine amide protons *d–g*) and aromatic axle proton *27*, tentatively attributed to differences in hydrogen bonding involving these protons (either intramolecularly and/or with the strongly hydrogen bond accepting DMSO solvent).

NMR experiments at elevated temperatures provided no evidence of dethreading of **6** or threading of **8**. However, they were used to study variation in the chemical shift of NH reso-
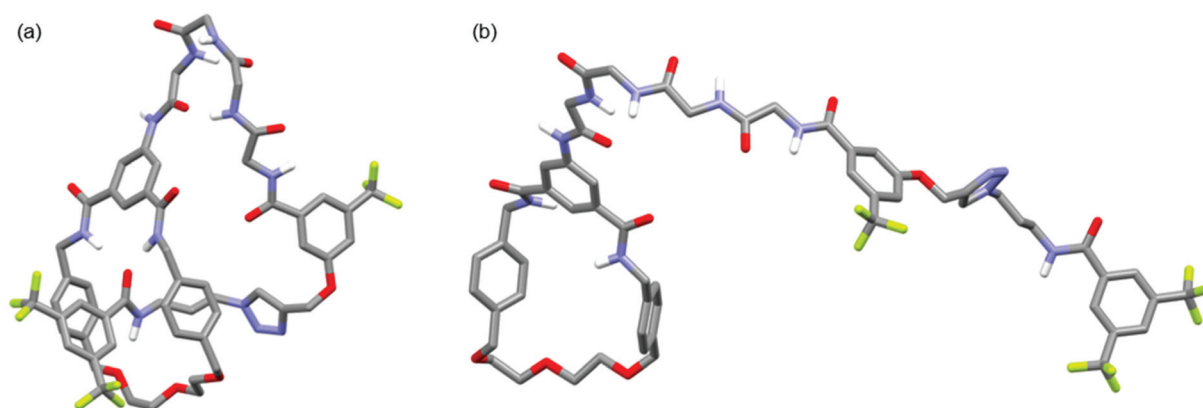
This journal is © The Royal Society of Chemistry 2020

Org. Biomol. Chem., 2020, **18**, 5203–5209 | **5205**

Fig. 4 Minimum energy DFT calculated structures of (a) [1]rotaxane **6** and (b) unthreaded isomer **8** (C−H hydrogen atoms omitted for clarity).

nances as a function of temperature, as has been used in the structural characterization of proteins in aqueous solution (see ESI, pages S45–S47‡).[17] In aqueous solution, temperature coefficients $\Delta\delta/\Delta T > -4.5$ ppb K^{-1} are attributed to intramolecular hydrogen bonds, while those that are more negative (<-4.5 ppb K^{-1}) are deemed to be freely interacting with solvent. The limited literature data for rigid peptides in D$_6$-DMSO is consistent with all coefficients being slightly less negative on average.[18]

For unthreaded **8**, all amide temperature coefficients are in the range -3.3 to -4.5 ppb K^{-1}, which is consistent with relatively unrestricted solvent accessibility. For [1]rotaxane **6**, the bulk of the NH environments have similar coefficients (in the range of -3.0 to -4.3 ppb K^{-1}) but there are two key exceptions. Axle amide *c* has a coefficient of -1.1 ppb K^{-1} implying it is inaccessible to solvent and macrocycle protons *b* have an unusually negative coefficient of -6.7 ppb K^{-1}. We attribute these deviations to the various non-covalent interactions arising from the axle component threading through the macrocycle cavity.

Further structural comparison between **6** and **8** was possible from ^{1}H diffusion NMR experiments (see ESI, pages S48 & S49‡).[19] For [1]rotaxane **6** the diffusion coefficient $D = 1.28 \pm 0.03 \times 10^{-10}$ m^2 s^{-1}, whereas for unthreaded analogue **8** $D = 1.10 \pm 0.03 \times 10^{-10}$ m^2 s^{-1}. In other words, the threaded [1]rotaxane diffuses faster which is consistent with a more compact 3D structure in solution. The observed D for both **6** and **8** is consistent with monomeric forms in solution,[20] and is also in agreement with a comparison of the DFT-simulated (B3LYP/6-31G*) structures of [1]rotaxane **6** and its unthreaded isomer **8** (Fig. 4).[21]

Conclusions

An expedient route to a peptide containing amide hydrogen bond templated [1]rotaxane has been demonstrated by the synthesis and structural characterization of a tetra-glycine containing [1]rotaxane. Looking forward, substitution of Boc–Gly–

Gly–Gly by other aliphatic side-chained peptide sequences should be straightforward, and in principle with modifications to protecting group strategy more exotic amino acid side-chains (or non-peptide motifs) could be incorporated. Hence delicate bioactive functionality could be displayed in the loop region, with protection against enzymatic degradation[9] and/or conformational control being provided by the entangled [1] rotaxane structure. Work on some of these avenues of research, as well as developing alternative synthetic routes to novel [1] rotaxanes, are ongoing in our laboratories.

Experimental

General information

Commercially available solvents and chemicals were used without further purification unless stated. Dry solvents, NEt$_3$ and DIPEA were purchased dry and stored under an inert atmosphere. Cu(CH$_3$CN)$_4$BF$_4$ was stored in desiccator over P$_4$O$_{10}$. Deionised water was used in all cases.

Silica gel with a 60 Å particle size was used as the stationary phase for column chromatography. Analytical TLC was used to monitor the progress of column chromatography and analytical TLC plates were examined under short wavelength ($\lambda = 254$ nm) UV light. Preparatory TLC was carried out on silica gel possessing a fluorescent indicator to allow for examination with short wavelength UV light.
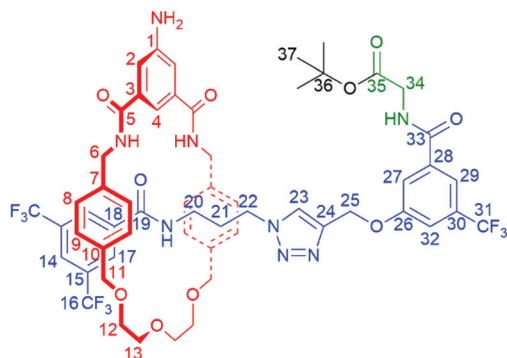
IR spectra of neat samples were recorded on an Agilent Technologies Cary 630 FTIR spectrometer. NMR spectra of samples dissolved in deuterated solvent were recorded on a Bruker AVANCE III 400 spectrometer at 298 K. 1D NMR spectra were referenced using residual solvent peaks, and assigned using standard ^{1}H–^{1}H COSY, ^{1}H–^{13}C HSQC and ^{1}H–^{13}C HMBC NMR experiments, with data being reported according to the atom labels as defined in the structures below. Electrospray mass spectra of dissolved samples, diluted in CH$_3$CN or CH$_3$OH, were recorded on a Shimadzu LCMS IT ToF instrument. Melting points were recorded on a Gallenkamp capillary melting point apparatus and are uncorrected.

Organic & Biomolecular Chemistry

Experimental procedures

[2]**Rotaxane 4.** Amino macrocycle **3** (107 mg, 0.219 mmol) and azide **1** (82 mg, 0.24 mmol) were dissolved in dry CH_2Cl_2 (10 mL) under an Ar (g) atmosphere. Then alkyne stopper **2** (86 mg, 0.24 mmol) in dry CH_2Cl_2 (1 mL), $Cu(CH_3CN)_4BF_4$ (7.6 mg, 0.024 mmol), TBTA (13 mg, 0.024 mmol) and DIPEA (34 mg, 46 μL, 0.26 mmol) were added. The reaction was stirred at r.t. for 15 h under an Ar (g) atmosphere. Then, the reaction was diluted to 20 mL, washed with 0.02 M EDTA in 1 M NH_3 (aq) solution (2 × 20 mL) and brine (1 × 20 mL). The organic layer was dried ($MgSO_4$) and solvent removed *in vacuo*. The crude material was purified by silica gel column chromatography (CH_2Cl_2/CH_3OH 99 : 1 to 96 : 4) to yield pure product **4** as a colourless film (52 mg). In addition, axle **7** (102 mg) was also isolated. Further pure product **4** was isolated after prep TLC of mixed fractions (17 mg). Total yield of [2]rotaxane **4**: 69 mg, 27%.

R_f: 0.20 (CH_2Cl_2/CH_3OH 98 : 2).

ν_{max}/cm^{-1} (neat): 3350 (N–H), 2920 (C–H), 1740 (C=O ester), 1650 (C=O amide), 1600, 1520, 1450, 1360, 1280, 1230, 1130, 1030.

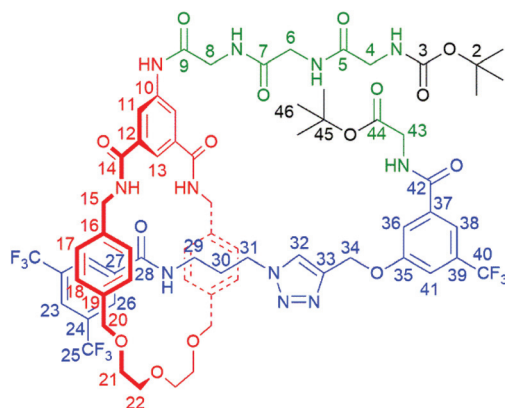δ_H (400 MHz; $CDCl_3/CD_3OD$ 1 : 1): 8.18 (2H, s, $C^{17}H$), 8.05 (1H, s, $C^{14}H$), 7.75–7.76 (2H, m, $C^{23}H$ & $C^{29}H$), 7.67 (1H, t, ^4J = 1.5 Hz, C^4H), 7.64 (1H, s, $C^{27}H$), 7.43 (1H, t, ^3J = 5.4 Hz, $C^{20}NH$), 7.36 (2H, d, ^4J = 1.5 Hz, C^2H), 7.32 (1H, s, $C^{32}H$), 6.88 (4H, d, ^3J = 7.9 Hz, C^8H), 6.71 (4H, d, ^3J = 7.9 Hz, C^9H), 5.02 (2H, s, $C^{25}H$), 4.49 (2H, d, ^2J = 14 Hz, C^6H – diastereotopic) 4.25–4.30 (4H, m, C^6H – diastereotopic & $C^{11}H$ – diastereotopic) 4.05–4.08 (4H, m, $C^{11}H$ – diastereotopic & $C^{34}H$), 3.99 (2H, t, ^3J = 7.0 Hz, $C^{22}H$), 3.54–3.72 (8H, m, $C^{13}H$ & $C^{12}H$), 2.67 (2H, br s, $C^{20}H$), 1.66–1.73 (2H, m, $C^{21}H$), 1.47 (9H, s, $C^{37}H$).

δ_C (100 MHz; $CDCl_3/CD_3OD$ 1 : 1): 170.0 (C^{35}), 168.7 (C^5), 167.9 (C^{33}), 165.0 (C^{19}), 159.4 (C^{26}), 149.1 (C^1), 143.1 (C^{24}), 138.1 (C^7), 137.1 (C^{10}), 137.1 (sic, C^{28}), 136.7 (C^{18}), 136.0 (C^3), 132.8 (q, ^2J = 32 Hz, C^{30}), 132.3 (q, ^2J = 34 Hz, C^{15}), 129.6 (C^9), 129.1 (C^{17}), 129.0 (C^8), 125.7 (C^{23}), 125.3 (br, C^{14}), 124.0 (q, ^1J = 271 Hz, C^{16}), 118.0 (C^2), 117.6 (br, C^{29}), 117.3 (C^{27}) 115.9 (br, C^{32}), 114.2 (C^4), 82.9 (C^{36}), 74.3 (C^{11}), 71.6 (C^{13}), 70.4 (C^{12}), 62.4 (C^{25}), 48.7 (C^{22}), 44.8 (C^6), 43.1 (C^{34}), 38.1 (C^{20}), 29.6 (C^{21}), 28.4 (C^{37}). Quartet for C^{31} lost in baseline.

δ_F (377 MHz; $CDCl_3/CD_3OD$ 1 : 1): −63.1 ($C^{16}F_3$), −63.4 ($C^{31}F_3$).

m/z (ES): 1209.4047 ([M + Na]$^+$ $C_{57}H_{59}F_9N_8NaO_{10}$ requires 1209.4103).

Boc-peptide [2]rotaxane 5. [2]Rotaxane **4** (69 mg, 0.058 mmol) was dissolved in dry CH_2Cl_2 (2 mL), and cooled to 0 °C under an Ar (g) atmosphere. Then dry NEt_3 (8.8 mg, 12 μL, 0.087 mmol), triglycine *tert*-butyl ester (17 mg, 0.058 mmol), HOBt·hydrate (10 mg, 0.076 mmol) and EDCI·HCl (15 mg, 0.076 mmol) were added, maintaining the temperature at 0 °C. The reaction was stirred at r.t. for 6 h, at which time analytical TLC confirmed presence of **4**. The reaction flask was cooled to 0 °C and further dry NEt_3 (8.8 mg, 12 μL, 0.087 mmol), triglycine *tert*-butyl ester (17 mg, 0.058 mmol), HOBt·hydrate (10 mg, 0.076 mmol) and EDCI·HCl (15 mg, 0.076 mmol) were added. The reaction was stirred at r.t. for a further 16 h, at which time analytical TLC confirmed presence of **4**. The reaction flask was cooled to 0 °C and further dry NEt_3 (8.8 mg, 12 μL, 0.087 mmol), triglycine *tert*-butyl ester (17 mg, 0.058 mmol), HOBt·hydrate (10 mg, 0.076 mmol) and EDCI·HCl (15 mg, 0.076 mmol) were added. The reaction was stirred at r.t. for a further 24 h, then diluted with CH_2Cl_2 (20 mL), and then washed with H_2O (1 × 20 mL), 10% citric acid (aq) (2 × 20 mL), saturated $NaHCO_3$ (aq) (2 × 20 mL) and brine (1 × 20 mL). The organic layer was dried ($MgSO_4$), and the solvent removed *in vacuo*. The crude material was purified by silica gel chromatography (CH_2Cl_2/CH_3OH 98 : 2 to 92 : 8) to yield pure product **5** as a white film (68 mg, 80%).

R_f: 0.22 (CH_2Cl_2/CH_3OH 96 : 4).

ν_{max}/cm^{-1} (neat): 3320 (N–H), 3070 (C–H), 2920 (C–H), 1650 (C=O), 1600, 1520, 1450, 1370, 1280, 1130, 1030.

δ_H (400 MHz; $CDCl_3$): 9.45 (1H, s, C^9NH), 8.19 (4H, s, $C^{11}H$ & $C^{26}H$), 8.07–8.10 (2H, br s, C^5HNH or C^7HNH & $C^{42}HNH$), 8.04 (1H, s, $C^{13}H$), 8.00 (1H, s, $C^{23}H$), 7.90 (1H, br s, C^5HNH or C^7HNH), 7.84 (2H, br s, $C^{14}NH$), 7.81 (1H, s, $C^{32}H$), 7.70 (1H, s, $C^{38}H$), 7.58 (1H, s, $C^{36}H$), 7.24 (2H, s, $C^{28}NH$ & $C^{41}H$), 6.94 (4H, d, ^3J = 7.9 Hz, $C^{17}H$), 6.74 (4H, d, ^3J = 7.9 Hz, $C^{18}H$), 6.28 (1H, br s, C^3HNH), 4.99 (2H, s, $C^{34}H$), 4.60–4.65 (2H, m, $C^{15}H$ – diastereotopic), 4.29 (2H, d, ^2J = 10 Hz, $C^{20}H$ – diastereotopic), 4.20–4.25 (2H, m, $C^{15}H$ – diastereotopic), 4.15 (2H, d, ^3J = 5.5 Hz, $C^{43}H$), 4.09 (2H, d, ^2J = 10 Hz, $C^{20}H$ – diastereotopic), 4.01 (6H, m, C^6H, C^8H & $C^{31}H$), 3.87 (2H, d, ^3J = 5.5 Hz, C^4H), 3.56–3.75 (8H, m, $C^{21}H$ & $C^{22}H$), 2.65–2.69 (2H,

Paper

app q, $C^{29}H$), 1.70–1.73 (2H, m, $C^{30}H$), 1.51 (9H, s, $C^{46}H$), 1.35 (9H, s, C^1H).

δ_C (**100 MHz; CDCl$_3$**): 171.9 (C^5), 170.7 (C^7 or C^9), 169.9 (C^{44}), 168.0 (C^7 or C^9), 166.8 (C^{14}), 166.2 (C^{42}), 164.0 (C^{28}), 158.5 (C^{35}), 156.7 (C^3), 142.1 (C^{33}), 138.8 (*), 137.3 (C^{16}), 136.2 (C^{19}), 136.0 (*), 135.8 (*), 135.1 (*), 131.4 (q, ^2J = 32 Hz, C^{24} and/or C^{39}), 128.8 (C^{18}), 128.3 (C^{17} & C^{26}), 124.8 (C^{32}), 124.5 (C^{23}), 123.1 (q, ^1J = 271 Hz, C^{25} and/or C^{40}), 121.6 (C^{11}), 120.3 (br, C^{13}), 117.0 (br, C^{38}), 116.4 (C^{36}), 115.0 (br, C^{41}), 82.7 (C^{45}), 80.1 (C^2), 73.6 (C^{20}), 70.8 (C^{22}), 69.5 (C^{21}), 62.0 (C^{34}), 47.7 (C^{31}), 44.5 (C^{15}), 44.3 (C^4), 43.7 (C^6 or C^8), 43.4 (C^6 or C^8), 42.8 (C^{43}), 37.3 (C^{29}), 28.7 (C^{30}), 28.2 (C^1), 28.1 (C^{46}). * = C^{10} or C^{12} or C^{27} or C^{37}.

δ_F (**377 MHz; CDCl$_3$**): −62.5 ($C^{25}F_3$), −62.7 ($C^{40}F_3$).

m/z (**ES**): 1480.5282 ([M + Na]$^+$ $C_{68}H_{76}F_9N_{11}NaO_{15}$ requires 1480.5271).

[1]Rotaxane 6. [2]Rotaxane **5** (20 mg, 0.014 mmol) was dissolved in CH$_2$Cl$_2$ (0.5 mL) and cooled to 0 °C. TFA (0.25 mL) was added dropwise and the reaction mixture was stirred at r.t. for 2 h. Volatiles were removed *in vacuo* and deprotection confirmed by ^{1}H NMR. The residue was re-dissolved in dry CH$_2$Cl$_2$ (7 mL), and cooled to 0 °C under an Ar (g) atmosphere. Then dry DIPEA (18 mg, 24 μL, 0.14 mmol) and HATU (16 mg, 0.042 mmol) were added, maintaining the temperature at 0 °C. The reaction was stirred at r.t. for 90 h, then diluted with CH$_2$Cl$_2$ to 20 mL, then washed with 1 M HCl (aq) (2 × 20 mL), sat. NaHCO$_3$ (aq) (2 × 20 mL) and brine (1 × 20 mL). The organic layer was dried (MgSO$_4$), and the solvent removed *in vacuo*. The crude material was purified by silica gel chromatography (CH$_2$Cl$_2$/CH$_3$OH 96 : 4 to 90 : 10) to yield pure product **6** as a white film (6.0 mg, 34%).

R_f: 0.31 (CH$_2$Cl$_2$/CH$_3$OH 94 : 6).

ν_{max}/cm^{-1} (**neat**): 3300 (N–H), 3080 (C–H), 2920 (C–H), 2870 (C–H), 1650 (C=O), 1600, 1530, 1450, 1360, 1330, 1280, 1170, 1130, 1030.

δ_H (**400 MHz; CDCl$_3$/CD$_3$OD 1 : 1**): 8.23 (2H, d, ^4J = 1.5 Hz, C^2H), 8.14 (1H, s, $C^{23}H$), 8.11 (2H, br s, $C^{17}H$), 8.02 (2H, app t, C^4H & $C^{14}H$), 7.65 (1H, s, $C^{29}H$), 7.38 (1H, s, $C^{27}H$), 7.15 (1H, s, $C^{32}H$), 6.91 (4H, d, ^3J = 8.0 Hz, C^8H), 6.76 (4H, d, ^3J = 8.0 Hz, C^9H), 4.83 (2H, s, $C^{25}H$), 4.60–4.62 (2H, obscured doublet, C^6H – diastereotopic), 4.30 (2H, d, ^2J = 10 Hz, $C^{11}H$ – diastereotopic),

4.19 (2H, s, $C^{34}H$), 4.12–4.17 (4H, m, $C^{22}H$ & C^6H – diastereotopic), 4.09 (2H, d, ^2J = 10 Hz, $C^{11}H$ – diastereotopic), 4.03 (2H, s, $C^{38}H$ or $C^{40}H$), 3.99 (2H, s, $C^{36}H$), 3.92 (2H, s, $C^{38}H$ or $C^{40}H$), 3.71–3.76 (2H, m, $C^{13}H$ – diastereotopic), 3.55–3.66 (6H, $C^{12}H$ & $C^{13}H$ – diastereotopic), 2.61 (2H, t, ^3J = 7.4 Hz, $C^{20}H$), 1.76–1.83 (2H, app quin, $C^{21}H$).

δ_C (**100 MHz; CDCl$_3$/CD$_3$OD 1 : 1**): 172.3 (C^{35}), 172.1 ($C^{37}/C^{39}/C^{41}$), 171.6 ($C^{37}/C^{39}/C^{41}$), 169.4 ($C^{37}/C^{39}/C^{41}$), 168.3 (C^5 & C^{33}), 164.7 (C^{19}), 159.2 (C^{26}), 142.9 (C^{24}), 139.3 (C^1 or C^3), 138.1 (C^7), 137.1 (C^{10}), 136.8 (C^{18} or C^{28}), 136.5 (C^{18} or C^{28}), 136.1 (C^1 or C^3), 132.7 (q, ^2J = 33 Hz, C^{30}), 132.2 (q, ^2J = 34 Hz, C^{15}), 129.4 (C^9), 128.9 (C^8 & C^{17}), 126.5 (C^{23}), 125.3 (br, C^{14}), 122.7 (C^2), 121.5 (C^4), 117.9 (br, C^{29}), 117.0 (C^{27}), 115.2 (br, C^{32}), 74.2 (C^{11}), 71.6 (C^{13}), 70.3 (C^{12}), 62.4 (C^{25}), 48.6 (C^{22}), 45.0 (C^6), 44.3 (C^{34}), 44.3 (sic, C^{38} or C^{40}), 43.8 (C^{38} or C^{40}), 43.6 (C^{36}), 37.8 (C^{20}), 29.5 (C^{21}). Quartets for C^{16} & C^{31} not fully resolved in 120–130 ppm region.

δ_F (**377 MHz; CDCl$_3$/CD$_3$OD 1 : 1**): −63.1 ($C^{16}F_3$), −63.5 ($C^{31}F_3$).

m/z (**ES**): 1306.3971 ([M + Na]$^+$ $C_{59}H_{58}F_9N_{11}NaO_{12}$ requires 1306.4015).

Conflicts of interest

There are no conflicts to declare.

Acknowledgements

Notes and references

1 For reviews about lasso peptides see: (*a*) M. O. Maksimov, S. J. Pan and A. J. Link, *Nat. Prod. Rep.*, 2012, **29**, 996–1006; (*b*) J. D. Hegemann, H. Zimmermann, X. Xie and M. A. Marahiel, *Acc. Chem. Res.*, 2015, **48**, 1909–1919; (*c*) H. Martin-Gómez and J. Tulla-Puche, *Org. Biomol. Chem.*, 2018, **16**, 5065–5080.

2 (*a*) R. A. Salomón and R. N. Farías, *J. Bacteriol.*, 1992, **174**, 7428–7435; (*b*) M. Iwatsuki, H. Tomoda, R. Uchida, H. Gouda, S. Hirono and S. Ōmura, *J. Am. Chem. Soc.*, 2006, **128**, 7486–7491; (*c*) T. A. Knappe, U. Linne, S. Zirah, S. Rebuffat, X. Xie and M. A. Marahiel, *J. Am. Chem. Soc.*, 2008, **130**, 11446–11454; (*d*) W. L. Cheung-Lee, M. E. Parry, A. J. Cartagena, S. A. Darst and A. J. Link, *J. Biol. Chem.*, 2019, **294**, 6822–6830.

5208 | *Org. Biomol. Chem.*, 2020, **18**, 5203–5209

This journal is © The Royal Society of Chemistry 2020

3 (a) R. Katahira, K. Shibata, M. Yamasaki, Y. Matsuda and M. Yoshida, *Bioorg. Med. Chem.*, 1995, **3**, 1273–1280; (b) T. A. Knappe, U. Linne, X. Xie and M. A. Marahiel, *FEBS Lett.*, 2010, **584**, 785–789.

4 (a) G. Helynck, C. Dubertret, J. F. Mayaux and J. Leboul, *J. Antibiot.*, 1993, **46**, 1756–1757; (b) N. R. Braddman, F. J. Piscotta, J. Hauver, E. A. Campbell, A. J. Link and S. A. Darst, *Proc. Natl. Acad. Sci. U. S. A.*, 2019, **116**, 1273–1278.

5 M. Chen, S. Wang and X. Yu, *Chem. Commun.*, 2019, **55**, 3323–3326.

6 T. A. Knappe, F. Manzenrieder, C. Mas-Moruno, U. Linne, F. Sasse, H. Kessler, X. Xie and M. A. Marahiel, *Angew. Chem., Int. Ed.*, 2011, **50**, 8714–8717.

7 Selected examples of synthetic [1]rotaxanes: (a) K. Hiratani, M. Kaneyama, Y. Nagawa, E. Koyama and M. Kanesato, *J. Am. Chem. Soc.*, 2004, **126**, 13568–13569; (b) Z. Xue and M. F. Mayer, *J. Am. Chem. Soc.*, 2010, **132**, 3274–3276; (c) H. Li, H. Zhang, Q. Zhang, Q.-W. Zhang and D.-H. Qu, *Org. Lett.*, 2012, **14**, 5900–5903; (d) H. Li, J.-N. Zhang, W. Zhou, H. Zhang, Q. Zhang, D.-H. Qu and H. Tian, *Org. Lett.*, 2013, **15**, 3070–3073; (e) B. Xia and M. Xue, *Chem. Commun.*, 2014, **50**, 1021–1023; (f) P. Waelès, C. Clavel, K. Fournel-Marotte and F. Coutrot, *Chem. Sci.*, 2015, **6**, 4828–4836; (g) Y. Wang, J. Sun, Z. Liu, M. S. Nassar, Y. Y. Botros and J. F. Stoddart, *Chem. Sci.*, 2017, **8**, 2562–2568; (h) A. Saura-Sanmartin, A. Martinez-Cuezva, A. Pastor, D. Bautista and J. Berna, *Org. Biomol. Chem.*, 2018, **16**, 6980–6987; (i) J.-J. Yu, L.-Y. Zhao, Z.-T. Shi, Q. Zhang, G. London, W.-J. Liang, C. Gao, M.-M. Li, X.-M. Cao, H. Tian, B. L. Feringa and D.-H. Qu, *J. Org. Chem.*, 2019, **84**, 5790–5802.

8 C. Clavel, K. Fournel-Marotte and F. Coutrot, *Molecules*, 2013, **18**, 11553–11575.

9 F. Saito and J. W. Bode, *Chem. Sci.*, 2017, **8**, 2878–2884.

10 B. E. Fletcher, M. J. G. Peach and N. H. Evans, *Org. Biomol. Chem.*, 2017, **15**, 2797–2803.

11 N. H. Evans and G. R. Akien, *Supramol. Chem.*, 2018, **30**, 758–764.

12 C. E. Gell, T. A. McArdle-Ismaguilov and N. H. Evans, *Chem. Commun.*, 2019, **55**, 1576–1579.

13 For a recent review on the hydrogen bond templated synthesis of rotaxanes (and catenanes) see: N. H. Evans, *Eur. J. Org. Chem.*, 2019, 3320–3343.

14 Selected examples of other, non-CuAAC click, stoppering of simple amide half-axles threaded through mono-isophthalamide macrocycles to generate [2]rotaxanes: (a) D. A. Leigh and A. R. Thomson, *Org. Lett.*, 2006, **8**, 5377–5379; (b) A. Vidonne and D. Philp, *Tetrahedron*, 2008, **64**, 8464–8475; (c) T. Kosikova, N. I. Hassan, D. B. Cordes, A. M. Z. Slawin and D. Philp, *J. Am. Chem. Soc.*, 2015, **137**, 16074–16083; (d) A. Vidonne, T. Kosikova and D. Philp, *Chem. Sci.*, 2016, **7**, 2592–2603.

15 The modest isolated yield of [2]rotaxane **4** is attributed to oxidation of the macrocyclic amino functionality, in particular during chromatographic purification.

16 HATU – (1-[bis(dimethylaminomethylene]-1*H*-1,2,3-triazolo[4,5-*b*]pyridinium oxide hexafluorophosphate) – is widely used for the macrocyclization of peptides. For reviews of this topic see: (a) C. J. White and A. K. Yudin, *Nat. Chem.*, 2011, **3**, 509–524; (b) Y. H. Lau, P. de Andrade, Y. Wu and D. R. Spring, *Chem. Soc. Rev.*, 2015, **44**, 91–102; (c) D. G. Rivera, G. M. Ojeda-Carralero, L. Reguera and E. V. Van der Eycken, *Chem. Soc. Rev.*, 2020, **49**, 2039–2059.

17 (a) N. J. Baxter and M. P. Williamson, *J. Biomol. NMR*, 1997, **9**, 359–369; (b) T. Cierpicki and J. Otlewiski, *J. Biomol. NMR*, 2001, **21**, 249–261.

18 M. Llinas and M. P. Klein, *J. Am. Chem. Soc.*, 1975, **97**, 4731–4737.

19 For reviews on the use of diffusion NMR experiments in supramolecular chemistry see: (a) S. V. Kharlamov and S. K. Latypov, *Russ. Chem. Rev.*, 2010, **79**, 635–653; (b) L. Avram and Y. Cohen, *Chem. Soc. Rev.*, 2015, **44**, 586–602.

20 R. Evans, Z. Deng, A. K. Rogerson, A. S. McLachlan, J. J. Richards, M. Nilsson and G. A. Morris, *Angew. Chem., Int. Ed.*, 2013, **52**, 3199–3202.

21 The DFT structure of [1]rotaxane **6** reveals that all amides in the loop (*a* & *d*–*g*) can be in a *trans* conformation. Depiction of amide *a* as *cis* in Scheme 1 arises from attempting to achieve a 2D depiction of [1]rotaxane **6** without unusual bond lengths or angles.

This journal is © The Royal Society of Chemistry 2020

Org. Biomol. Chem., 2020, **18**, 5203–5209 | **5209**